EurJIC
European Journal of Inorganic Chemistry

Research Article
doi.org/10.1002/ejic.202500286

Chemistry Europe
European Chemical Societies Publishing

www.eurjic.org

Variable Coordination of Peroxide in a Dinuclear Copper Mono-Oxygenase Model Complex Supported by a Pyridazine-Bridged Ligand

Alexander Stüber, Ramona Jurgeleit, Kira Berger, Benjamin Grimm-Lebsanft, Sören Buchenau, Laura Senft, Christian Näther, Ivana Ivanović-Burmazović, Michael Rübhausen,* Maria A. Naumova,* and Felix Tuczek*

Dedicated to Prof. Dr. Christian Limberg and to Prof. Dr. Franc Meyer on the occasion of their 60th birthdays

Copper-oxygen intermediates play an important role in nature as active species of many copper-containing enzymes. However, copper-oxygen intermediates have a key function not only in nature, but also in industry, for example as catalysts. Herein a study on a dinuclear copper complex is presented based on the literature known ligand **BPMPD**. This ligand combines features of the previously investigated systems (octadentate *N*-donor, like the **MO8** system and pyridine donors, like the **bdpdz** system). Oxygenation of the Cu(I)-complex with O_2 at low temperature leads to the formation of a μ-1,2-peroxo intermediate (**Cu_2O_2**), which is characterized with UV/Vis-, rRaman- and X-ray absorption spectroscopy (XAS), as well as by cryo-UHR-electrospray ionization mass spectrometry. The **Cu_2O_2** species can be reversibly converted into a μ-1,1-hydroperoxo intermediate (**Cu_2OOH**) by a reaction with lutidinium triflate and 1,8-diazabicyclo[5.4.0]undec-7-ene (DBU), which can be monitored by UV/Vis and XAS. Furthermore, the reactivity of the **Cu_2O_2** species toward dihydroanthracene is investigated.

1. Introduction

Cu_2O_2 cores mediate a number of essential processes in nature, such as oxygen transport in mollusks and arthropods (hemocyanin) or the oxygenation of phenols for the synthesis of the biopolymer melanin (tyrosinase) via a μ-η^2:η^2-peroxodicopper(II) complex.[1–4] **Cu_2O** intermediates, on the contrary, play a role in the oxygenation of hydrocarbons, such as in the zeolite Cu-ZSM-5 which can convert methane to methanol after activation with O_2.[5–7] There are numerous examples of copper complexes serving as catalysts for the oxidation of hydrocarbons,[8] alcohols,[9] phenols,[10] catechols[11] and other organic substrates in homogeneous solution via **Cu_xO_y** intermediates.[12] In 2021, we published a study about copper complexes supported by the hexadentate pyridazine- and phthalazine-based ligands **bdpdz**[13] and **bdptz,**[14] respectively, in which a mixed-valent $Cu(I)_2Cu(II)_2$ μ_4-peroxo species is formed after reaction of a Cu(I) precursor with O_2 at 193 K. Warming to 233 K lead to homolytic O—O bond cleavage, generating a **Cu_2O** species that is able to oxygenate hydrocarbons with a BDE of up to 82 kcal mol^{-1}.[15] Recently, we replaced the hexadentate by an octadentate ligand and introduced terminal pyrazole instead of pyridine donors in the side arms, resulting in the **MO8** system.[16] Through this modification of the ligand design, the **Cu_2O** intermediate was found to be unstable in the **MO8** system, and a μ-1,1-hydroperoxo dicopper(II) (**Cu_2OOH**) species was detected upon oxygenation at 193 K. Room temperature oxygenation, on the contrary, was found to lead to a dihydroxo dicopper(II) complex **$Cu_2(OH)_2$**. In line with the lack of formation of the highly active **Cu_2O** species, the **MO8** system also exhibits a significantly lower reactivity toward hydrocarbons than the **bdpdz/bdptz** systems; that is, only anthrone (BDE = 76 kcal mol^{-1})[17] could be converted to anthraquinone.[16]

A. Stüber, R. Jurgeleit, K. Berger, C. Näther, F. Tuczek
Institute of Inorganic Chemistry
Christian-Albrechts-University of Kiel
Max-Eyth-Straße 2, 24118 Kiel, Germany
E-mail: ftuczek@ac.uni-kiel.de

B. Grimm-Lebsanft, S. Buchenau, M. Rübhausen
Institut für Nanostruktur- und Festkörperphysik
Center for Free Electron Laser Science (CFEL)
Universität Hamburg
Luruper Chaussee 149, 22761 Hamburg, Germany
E-mail: mruebhau@physnet.uni-hamburg.de

L. Senft, I. Ivanović-Burmazović
Department Chemie
Ludwig-Maximilians-Universität München
Butenandtstrasse 5-13, Haus D, 81377 München, Germany

M. A. Naumova
DESY, Deutsches Elektronen-Synchrotron (DESY)
Notkestrasse 85, 22607 Hamburg, Germany
E-mail: maria.naumova@desy.de

Supporting information for this article is available on the WWW under https://doi.org/10.1002/ejic.202500286

Research Article
doi.org/10.1002/ejic.202500286

Chemistry Europe
European Chemical Societies Publishing

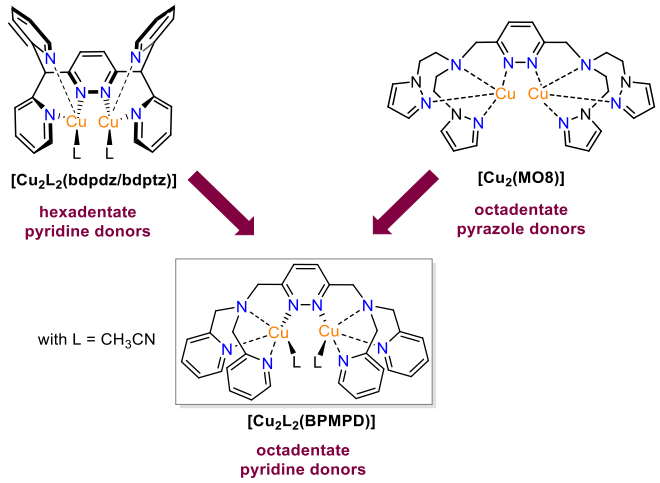

Scheme 1. The [Cu_2L_2(**BPMPD**)] complex (L = CH_3CN) combines structural features of the previously investigated **MO8** and the **bdpdz** systems.

Pursuing further our studies on dicopper complexes supported by dinucleating ligands with a pyridazine bridge, we herein investigate copper coordination of the recently published bis(pyridylmethyl)amine-pyridazine (**BPMPD**) ligand,[18] which is octadentate as **MO8** and exhibits the same backbone. In contrast to **MO8**, however, this ligand has terminal pyridine donors in the side arms, similar to the **bdpdz** system (see **Scheme 1**).[15,16,18] Whereas the Cu(II) complex of **BPMPD** has been studied with respect to water oxidation,[18] we are interested in exploring the reactivity of the (so far unknown) Cu(I) **BPMPD** complex toward dioxygen and its monooxygenase activity. Shortening the C_2–C_1 bridges in the side arms and replacing the terminal pyrazole by pyridine groups should lead to changes in the geometric and electronic structure with respect to the **MO8** system and thus significantly influence the stabilization of Cu_2O_x intermediates.

In this study, we synthesize the copper(I) complex [Cu_2(**BPMPD**)$(CH_3CN)_2$]X_2 (X = PF_6, OTf) and investigate its reactivity toward O_2 using UV/Vis-, rRaman-, XAS as well as by cryo-UHR-electrospray ionization mass spectrometry (ESI-MS), identifying differences to the **MO8** and **bdpdz** systems. In addition, the monooxygenation activity of the Cu_2-**BPMPD** system toward the organic substrate dihydroanthracene is tested and compared with the reactivities of the previously investigated systems.

2. Results and Discussion

2.1. Synthesis and Structural Characterization

2.1.1. Synthesis of the Ligand 1 and the Dicopper(I) Complex 2

In contrast to the literature-known synthesis of **BPMPD**,[18] we prepared this ligand in analogy to the route applied to the synthesis of **MO8**,[16] resulting in a significantly simpler access. As for **MO8**, we first synthesized 3,6-bis(chloromethyl)-pyridazine (**BCMPydz**), which forms the pyridazine backbone of the ligand. Reaction of this compound with bis(2-pyridylmethyl)amine (**BPMA**) leads to the ligand **BPMPD** (**1**; **Scheme 2**).[19] Complexation of **1** with copper (II) nitrate in acetone/ dichloromethane (1:1) led to a green product (Section S2.3.3). Slow evaporation of the solution afforded single crystals of the composition $([Cu_2(\mathbf{BPMPD})(NO_3)_3]^+)_4$ $[Cu(NO_3)_4]^{2-}$ $(NO_3^-)_2$ which were subjected to XRD. The structure of the complex cation proves the constitution of the ligand (Figure S1, Supporting Information).[20] Furthermore, the obtained Cu—N bond lengths are in agreement with those determined for the Cu(II) complex [Cu_2(**BPMPD**)(OH)] (**Cu_2OH**; see below).[18]

In analogy to the previously investigated **bdpdz** and **MO8** systems,[15,16] Cu(I)-complexes **2**-X of **BPMPD** were obtained by reaction of the free ligand with two equivalents of $[Cu(CH_3CN)_4]X$ (X = PF_6, OTf) in acetonitrile (Scheme 2).[19,20]

For comparison and further investigation, we reproduced the **Cu_2OH** complex **5**-ClO_4 according to ZHANG et al.[18] The **Cu_2OH** complex exhibits three absorption bands in the UV/Vis spectrum at 360 nm ($\varepsilon = 5500\ M^{-1}\ cm^{-1}$), 655 nm ($\varepsilon = 130\ M^{-1}\ cm^{-1}$) and 830 nm ($\varepsilon = 280\ M^{-1}\ cm^{-1}$) similar to the **MO8** system (Figure S21, Supporting Information). The IR spectrum shows band at 3495 cm^{-1} that can be assigned to the O—H vibration of the hydroxido ligand, as for the **MO8** system (Figure S27, Supporting Information).[16] The ESI mass spectrum has a great similarity to the spectrum obtained by ZHANG and shows [**Cu_2(BDMPD)OH**]$^{3+}$ as the main species (Section S6.1).[18] In the ^{1}H-NMR spectrum, the signals are strongly shifted downfield and show strong paramagnetic broadening due to the presence of Cu(II), which makes assignment difficult. However, the number of signals matches the expected value (Figure S15, Supporting Information). Because of the broadening, no signals are visible in the ^{13}C-NMR spectrum in analogy to the **Cu_2OH** complex of the **MO8** system (Figure S16, Supporting Information).[16]

2.2. Exploring Copper-Oxygen Intermediates of the Cu_2-BPMPD System with Density Functional Theory (DFT)

In order to obtain an impression of the capability of the Cu_2-**BPMPD** system to support various Cu_2O_x intermediates,

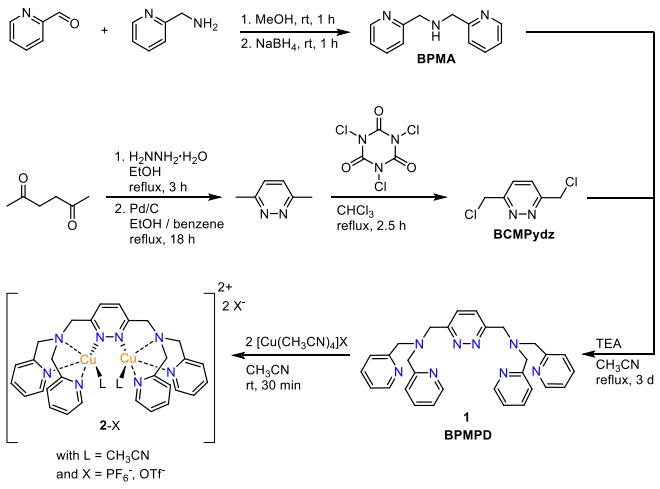

Scheme 2. Synthesis of the ligand **BPMPD** and the corresponding Cu(I)-complex **2**-PF_6 and **2**-OTf.

Research Article
doi.org/10.1002/ejic.202500286

DFT was employed. For a calibration of these calculations, we first considered the μ-hydroxo dicopper (II) complex (**Cu_2OH**), which was structurally characterized by ZHANG et al.[18] (**Figure 1**). The experimentally determined structure of **Cu_2OH** was well reproduced by the calculation, and the bond lengths and angles of the theoretically determined structure were found to be in good agreement with the crystal structure (Table S6, Supporting Information).

We then carried out geometry optimizations of various possible **Cu_2O_x** intermediates (**Cu_2O**, end-on/side-on **Cu_2O_2**, bis-μ-oxo **Cu_2O_2**, **Cu_2OOH**, **$Cu_2(OH)_2$**) of the **BPMPD** system. Based on the calculations and the crystal structure, it is most likely that an intermediate is present in which the two copper centers are each pentacoordinated (**Cu_2O**, **Cu_2OH**, end-on **Cu_2O_2**, **Cu_2OOH**). Our recently published **MO8** system also exhibits a pentacoordinate environment for the **Cu_2OH** and **Cu_2OOH** complexes.[16] The geometry-optimized structures of the **Cu_2O**, end-on **Cu_2O_2** and **Cu_2OOH** complexes are shown in **Figure 2**.

Importantly, the calculated structures in which the Cu(II) centers are hexacoordinated (side-on **Cu_2O_2**, bis-μ-oxo **Cu_2O_2** and **$Cu_2(OH)_2$**, see Figure S59–S61, Supporting Information) lead to strong distortions of the systems and, in particular, result in strongly elongated Cu—N bonds. We therefore consider it unlikely that any of these structures are formed in the Cu_2-**BPMPD** system.

It should be mentioned that geometry optimization of the copper(I) complex led to reasonable structures both with and without acetonitrile coligands (cf Figure S54, Supporting Information). Experimentally, the data of the Cu(I) complex **2**-PF_6 (cf Section S2.3), however, suggest that acetonitrile coordinates to copper as a coligand. In the ^{1}H-NMR-spectrum is a singlet at 1.96 ppm that indicates the presence of coordinated acetonitrile. With the **bdpdz**/**bdptz** system, which exhibits two acetonitrile coligands, we observed a signal on the same shift.[15] In addition, the integral would match two acetonitrile molecules. Furthermore, the elemental analysis of **2**-PF_6 matches a complex that has two acetonitrile coligands. Additional evidence for the presence of acetonitrile is provided by liquid IR spectroscopy measured in dichloromethane. Two small bands at 2293 and 2255 cm^{-1} are visible, which can be assigned to the C—N vibration of acetonitrile (Figure S26, Supporting Information).[21] However, the coligands seem to be only weakly bound, as they are not visible with ESI-MS and XAS.

2.3. Generation and Characterization of the μ-1,2 Peroxo Complex

2.3.1. UV/Vis Spectroscopy

Upon oxygenation of the orange solution of **2**-PF_6 at 183 K, the color turned dark blue/purple. The resulting absorption bands at 360 ($\varepsilon = 3500$), 450 ($\varepsilon = 1500$), 550 ($\varepsilon = 1600$) and at 620 nm ($\varepsilon = 1600\ M^{-1}\ cm^{-1}$) were most pronounced at 203 K (**Figure 3**, red). The band positions and intensities are in good agreement with literature-known μ-1,2 peroxo complexes (**Cu_2O_2**), and a purple color has also been observed for this type of copper-oxygen intermediate.[2,22–28] Therefore we assign this species as a **Cu_2O_2** complex (**3**). The bands at 550 and 620 nm can be assigned to π^* (peroxide) $\rightarrow$ d (Cu(II)) ligand-to-metal charge transfer (LMCT) transitions.[22] The shoulder at 450 nm is also present in spectra of other trans μ-1,2 peroxo dicopper complexes,[22,25] but might also originate from a superoxo species, which is in equilibrium with the μ-1,2 peroxo complex.[29–31] Absorption bands between 400–450 nm were observed for dicopper superoxo complexes in the literature.[29–33]

Warming of the solution leads to a rapid intensity decrease of the bands and disappearance of the blue/purple color (Figure S18, Supporting Information). In contrast to these observations, the **bdpdz** system was found to form a green-colored tetranuclear μ_4-peroxide $Cu(I)_2Cu(II)_2$ complex with O_2 at −90 °C which is transformed to a **Cu_2O** species upon warming to −40 °C.[15] For the **MO8** system, on the contrary, oxygenation with O_2 at −90 °C generates a **Cu_2OOH** complex.[16]

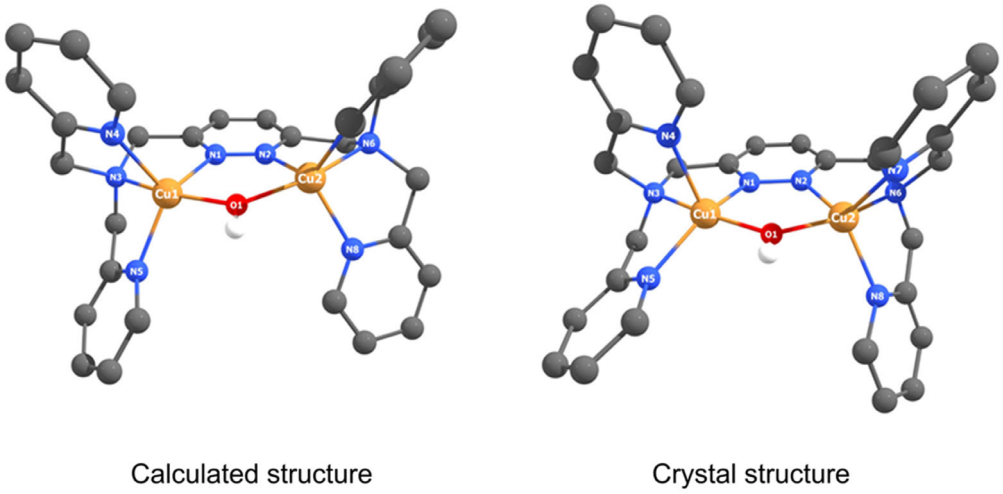

Figure 1. Geometry optimization of the **Cu_2OH** complex (left) and crystal structure of the **Cu_2OH** complex obtained by ZHANG et al.[18] (right). All hydrogen atoms attached to carbon are omitted for clarity. DFT: RI-PBE-D3(BJ)/def2-SVP.

Research Article
doi.org/10.1002/ejic.202500286

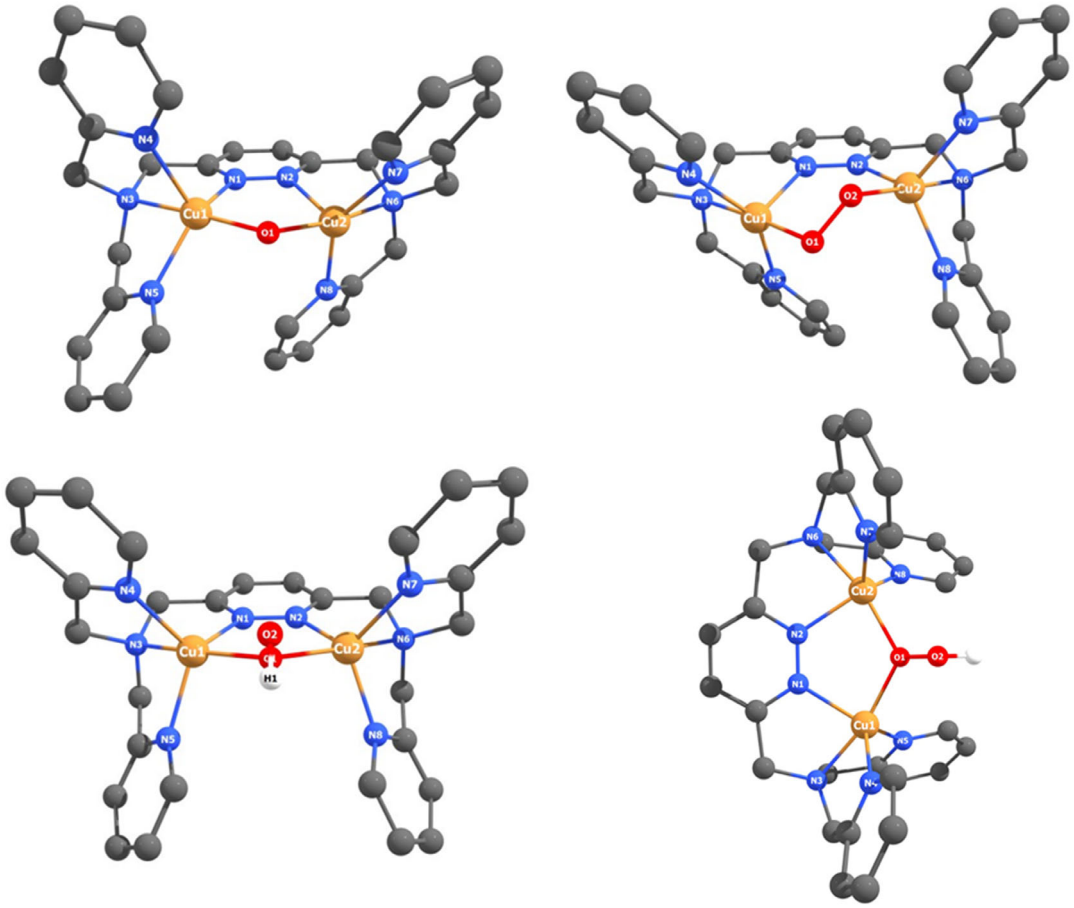

Figure 2. Geometry optimizations of the, **Cu_2O** (top left), μ-1,2 **Cu_2O_2** (top right) and **Cu_2OOH** complex in two perspectives (bottom). All hydrogen atoms attached to carbon are omitted for clarity. DFT: RI-PBE-D3(BJ)/def2-SVP.

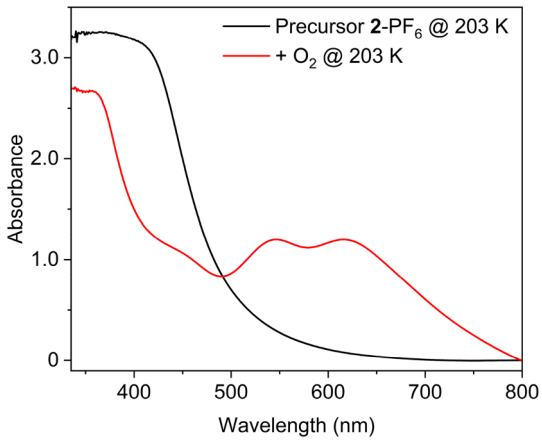

Figure 3. UV/Vis spectrum of an acetone solution of **2**-PF_6 (black) and spectrum obtained after reaction with O_2 at 190 K (red).

2.3.2. rRaman

Resonance Raman spectroscopy was employed to confirm the presence of the μ-1,2 peroxo species **3**. To this end we used a wavelength of 532 nm for irradiation and carried out oxygenation reactions of **2**-PF_6 with $^{16}O_2$ and $^{18}O_2$ at 203 K. The oxygenation experiments revealed the presence of two isotope-sensitive peaks at 507 ($\Delta = 23$) and 807 cm^{-1} ($\Delta = 45$ cm^{-1}) (**Figure 4**). The peak at 807 cm^{-1} and the corresponding isotopic shift can be assigned to an O—O vibration and are in good agreement with literature data for μ-1,2 peroxo complexes.[22–26,28] In addition, the peak at 507 cm^{-1} and the corresponding isotope shift match the literature data for Cu—O vibrations in μ-1,2 peroxo complexes.[22,24] DFT calculations predict an O—O vibration at 1087 cm^{-1} ($\Delta = 62$ cm^{-1}), a symmetric Cu—O vibration at around 363 cm^{-1} ($\Delta = 9$ cm^{-1}) and an antisymmetric Cu—O vibration at around 382 cm^{-1} ($\Delta = 15$ cm^{-1}) for this system. The Raman data obtained thus confirm our assumption of a μ-1,2 peroxo species, in agreement with the UV/Vis data.

2.3.3. XAS

To obtain detailed information on the environment and the oxidation state of the copper, we investigated the reaction of **2**-PF_6 with O_2 at 203 K using XAS.[34] For the XAS experiment, a 20.1 mM solution of **2**-PF_6 was used. X-ray absorption near-edge structure (XANES) spectrum of the complex **2**-PF_6 is similar to spectra of **MO8** and **bdpdz**/**bdptz** and agrees with the Cu(I) character (**Figure 5** (black), Figure S51, Supporting Information).[15,16]

Research Article
doi.org/10.1002/ejic.202500286

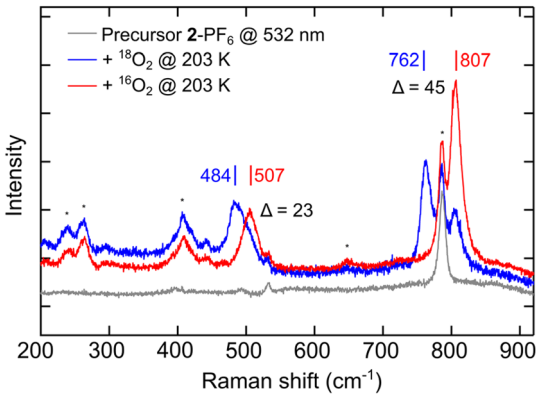

Figure 4. Resonance Raman spectrum of **2**-PF_6 (gray) and spectra obtained after reaction with $^{16}O_2$ (red) and $^{18}O_2$ (blue) at 203 K, generating **3**-PF_6. The solvent signals of the acetone are marked with asterisks.

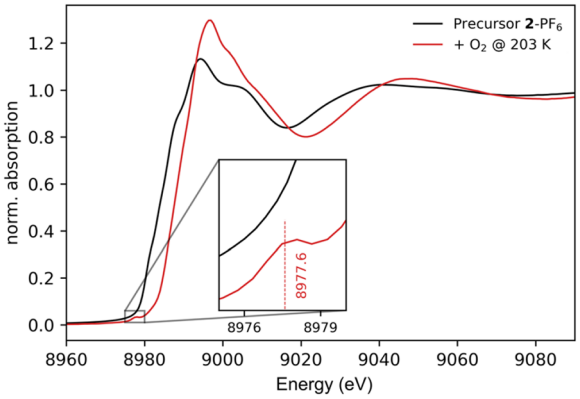

Figure 5. Cu K-edge XANES spectra of the precursor **2**-PF_6 (black) and the μ-1,2 Cu_2O_2 complex **3**-PF_6 (red) obtained after reaction with O_2 at 203 K with enlarged preedge region.

The edge position measured at 50% of the edge jump (*E*½) is at 8983.8 eV. The shoulder at 8981.2 eV is weaker than in the spectra of **MO8** and **bdpdz/bdptz** systems, while a shoulder at 8987.6 eV is quite pronounced.[15,16] The XANES spectrum of the dark blue/purple **3**-PF_6 solution indicates the presence of Cu(II) (Figure 5, red): the edge position is shifted to a higher energy (*E*½ = 8987.5 eV) and there is a preedge peak at 8977.6 eV, which is characteristic for Cu(II).

Extended X-ray absorption fine structure (EXAFS) spectrum of **2**-PF_6 and **3**-PF_6 could be fitted using the geometry-optimized structures as models, for details, see (Section S6, Figure S53, Supporting Information).

Thus, UV/Vis, Raman, and XAS data strongly support the conclusion that the low-temperature Cu_2O_x intermediate in the **BPMPD** system is a μ-1,2 peroxo species.

2.3.4. Cryo-UHR-ESI-MS

To further complement our spectroscopic data, we investigated the reaction of **2**-PF_6 with O_2 at 203 K by means of Cryo-UHR-ESI-MS. Contrary to our expectations, however, the Cu_2O_2 species was not visible in the mass spectrum. A reason for this may be the high thermal instability of this species, which we already observed in the low-temperature UV/Vis experiment (see above). Decay of this species might also have occurred during the very short period of transfer of the solution to the mass spectrometer. By contrast, a $[Cu_2(BPMPD)O]^{2+}$ intermediate (*calc. m/z* 322.0562, *obs. m/z* 322.0568) was found as the main species in the mass spectrum. In addition, a $[Cu_2(BPMPD)OH]^{3+}$ species (*calc. m/z* 215.0399, *obs. m/z* 215.0393) could be detected. Finally, the "bare" Cu(I) complex $[Cu_2(BPMPD)]^{2+}$ (*calc. m/z* 314.0587, *obs. m/z* 314.0586) as well as a $[Cu(I)Cu(II)(BPMPD)]^{3+}$ species (calc. m/z 209.3723, obs. m/z 209.0366) were observed (Figure S39–S42, Supporting Information).

2.3.5. Reactivity Experiments

The Cu_2O_2 species **3** was tested regarding its reactivity toward the substrate dihydroanthracene (DHA, BDE = 78 kcal mol^{-1}).[35] Notably, the **bdpdz/bdptz** system was able to catalytically convert DHA to anthraquinone (AQ) with a TON of 5, but for the **MO8** system no reactivity toward this substrate was observed.[15] In the first experiment, the reaction was carried out with 5 eq. DHA for 6 h at 203 K, whereby AQ with a conversion of 6.6% (TON = 0.17) was obtained. In the second experiment, the reaction mixture was warmed up to rt after 6 h at 203 K and left at this temperature for 18 h. In this case AQ with a yield of 14.1% (TON = 0.35) could be obtained. Control experiments with the Cu(I) precursor and in the absence of copper showed no conversion at all (see **Table 1**). Regarding C—H activation, the **BPMPD** system is therefore more reactive than **MO8**, but significantly less reactive than **bdpdz/bdptz**.

2.4. Protonation of the Cu_2O_2 Species 3

In the next step we investigated whether the μ-1,2 peroxo complex of the **BPMPD** system can be reversibly protonated. For this purpose, we used the acid 2,6-lutidinium triflate ([Lut-H][OTf]) to protonate the Cu_2O_2 complex and diazabicycloundecene (DBU) for deprotonation of the resulting species. It is known from the literature that protonation of Cu_2O_2 complexes may lead to μ-1,1-hydroperoxo dicopper(II) complexes (Cu_2OOH).[2,22,26,31,36,37] Therefore, we wanted to check whether the Cu_2O_2 species **3** also behaves in this manner (**Scheme 3**). It should be mentioned that the μ-1,2 peroxo species could possibly be in equilibrium with a μ-1,1 peroxo species that undergoes protonation at the terminal oxygen atom, leading to a μ-1,1 hydroperoxo dicopper (Cu_2OOH) complex. DFT calculations of the μ-1,1 peroxo dicopper species suggest that such an intermediate may be stable for the **BPMPD** system (Section S9.9). The protonation and deprotonation reaction of the Cu_2O_2 complex **3** were monitored by means of UV/Vis-spectroscopy and XAS.

2.4.1. UV/Vis

For the protonation reaction, 1.2 eq. of the acid lutidinium triflate [H–Lut][OTf] were added to a solution of the Cu_2O_2

Research Article
doi.org/10.1002/ejic.202500286

Table 1. Reactivity of **3**-PF_6 toward dihydroanthracene.

System	Conversion
3-PF_6, 203 K, 6 h	7%
3-PF_6, 203 K, 6 h, and rt for 18 h	14%
$[Cu(CH_3CN)_4]PF_6$ 203 K, O_2, 6 h, and rt for 18 h	0%
No Cu, 203 K O_2, 6 h, and rt for 18 h	0 %

complex **3** in acetone at 173 K, which led to a color change from blue to green within a few seconds. Correspondingly, four new absorption bands appeared in the UV/Vis spectrum at 370 ($\varepsilon = 4600$), 400 ($\varepsilon = 4000$), 620 ($\varepsilon = 65$) and 810 nm ($\varepsilon = 90\ M^{-1}\ cm^{-1}$) (**Figure 6**, green and S25, Supporting Information). The UV/Vis bands are in good agreement with those reported for **Cu_2OOH** complexes in the literature.[2,22,26,27,36–40] Moreover, they are strikingly similar to a **Cu_2OOH** complex supported by a pyrazolate-bridged dinucleating ligand which could be reversibly generated by protonation of the μ-1,2 **Cu_2O_2** complex and exhibited UV/Vis bands at 416 nm (with a shoulder at 367 nm) and 605 nm.[26] We thus conclude that we have obtained the μ-1,1 hydroperoxo dicopper (**Cu_2OOH**) complex **4** after protonation (Scheme 3). The UV/Vis bands at 367 and 401 nm have been assigned to hydroperoxo LMCT transitions and the band at 623 nm to a Cu(II) *d-d* transition.[26,41] Based on the amount of the **Cu_2OOH** complex formed after addition of 1.0 eq. [Lut-H][OTf], we tried to estimate a pK_a value for the **Cu_2OOH** complex (Section S3.2). The estimation resulted in a pK_a between 6.49 and 8.78 depending on the solvent (about two units higher than that of [Lut-H][OTf]).

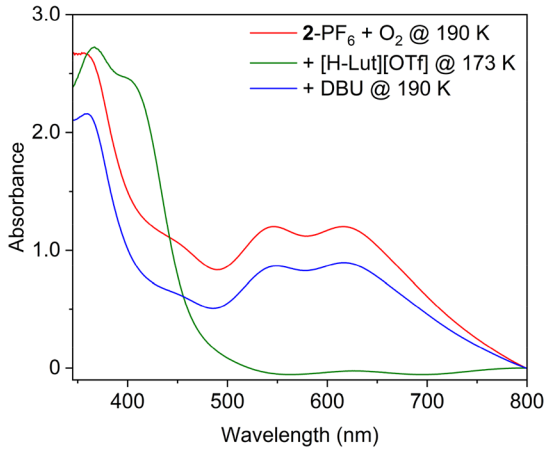

Figure 6. UV/Vis spectroscopic investigation of the protonation experiment. UV/Vis spectrum of an acetone solution of **2**-PF_6 after oxygenation (red), after addition of 1.2 eq. [Lut-H][OTf] (green) and after the subsequent addition of 1.4 eq. DBU (blue).

As described in the literature for other **Cu_2OOH** complexes, the **Cu_2OOH** complex **4** can also be obtained by reaction of the **Cu_2OH** complex **5** with H_2O_2 at low temperatures (Scheme 3 and Figure S22, Supporting Information).[22,36,38,39]

When 1.4 eq of the base diazabicycloundecene (DBU) was added, the solution turned dark blue/purple again. A UV/Vis spectrum was obtained that matched that of the original **Cu_2O_2** complex (Figure 6, blue). Thus, the **Cu_2O_2** complex can be reversibly protonated in analogy to earlier examples in the literature.[26,31]

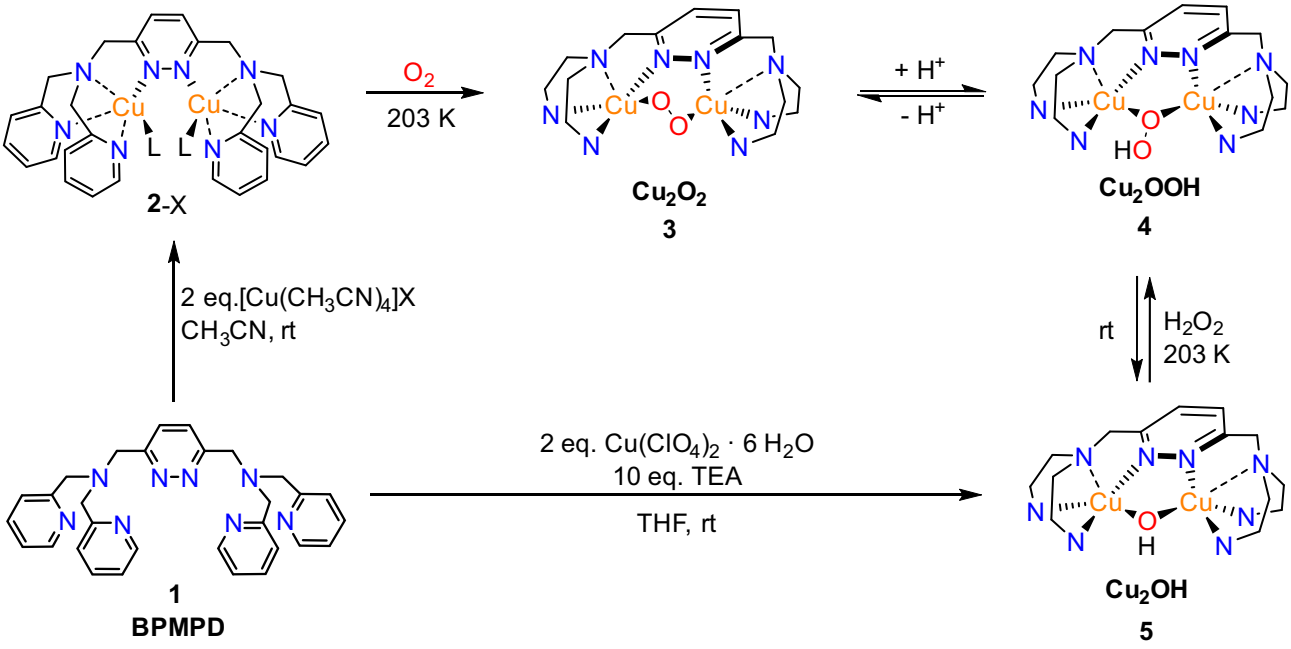

Scheme 3. Reversible protonation of the **Cu_2O_2** complex **3**. First, the reaction of the Cu(I) complex **2**-X (with X = PF_6^- or OTf^- and L = CH_3CN) with O_2 at 203 K leads to the μ-1,2-peroxo species **3** (**Cu_2O_2**, middle). Protonation of this species (for example with [Lut-H][OTf]) leads to a μ-1,1-hydroperoxo species **4** (**Cu_2OOH**, right), which can be converted back to the **Cu_2O_2** complex by deprotonation (for example with DBU). Warming the **Cu_2OOH** species to rt leads to the **Cu_2OH** complex **5**. Starting from the **Cu_2OH** complex, the **Cu_2OOH** complex can be obtained by reaction with H_2O_2 at 203 K.

Research Article
doi.org/10.1002/ejic.202500286

2.4.2. XAS

As in the XAS experiment described in Section 3, a 20.1 mM solution of **2**-PF_6 was first reacted with O_2 at 203 K to form **3**-PF_6. After the addition of 1.2 eq [Lut-H][OTf] to generate **4**-PF_6, the color of the solution changed to green after a short time, as observed in the UV/Vis experiment. The XANES spectrum obtained for **4**-PF_6 confirms that a Cu(II) species is present as expected (**Figure 7**, blue, and Figure S51, Supporting Information). Compared to **3**-PF_6, the edge position of **4**-PF_6 is shifted by 0.15–0.25 eV to higher energy ($E½ = 8987.65$ eV), and the preedge peak remains at 8977.6 eV. In the EXAFS spectrum, the amplitudes of the oscillations become stronger for **4**-PF_6 compared to **3**-PF_6, while their frequencies do not really change (Figure S52, Supporting Information). The EXAFS spectrum of **4**-PF_6 could be fitted to the geometry-optimized **Cu_2OOH** structure, for details, see (Section S8, Figure S53, Supporting Information); the fitted Cu—Cu distance is 3.35 Å (DFT model: 3.48 Å). Subsequently, 1.4 eq. DBU was added, resulting in a dark blue/purple color of the solution. The XANES spectrum (Figure 7, green; Figure S51, Supporting Information) shows return of the edge position back to that of **3**-PF_6, with additional appearance of a minor amount of Cu(I) character (further shift of the edge at 8983–8987 eV to the lower energy and reduction of the peak at 8997 eV). Thus, it could also be shown by XAS that the protonation of the μ-1,2 peroxo complex is reversible.

In contrast to the **Cu_2OOH** complex, the XAS fit of the **Cu_2O_2** complex didn't show sensitivity to the Cu—Cu distance. Nevertheless, the XAS fit indicates that the first shell (which consists of N and O atoms) around Cu barely changes upon protonation. Notably, the DFT calculations show that the Cu—Cu distance of the μ-1,2 peroxo species (3.669 Å) is only 0.2 Å longer than calculated for the **Cu_2OOH** complex (3.447 Å) (Section S9). As a matter of fact, the calculated Cu—Cu distance of the former is very short, even shorter than observed for the above-mentioned peroxo complex supported by a pyrazolate-bridged dinucleating ligand (3.797 Å).[25]

2.5. Attempt to Generate a μ-Oxo Dicopper(II) Species

As already mentioned, warming up the **Cu_2O_2** species leads to decomposition of the complex. This implies that, unlike the **bdpdz** system, a **Cu_2O** species is not accessible from reaction of the Cu(I) complex with O_2 in this way. Since the geometry optimizations of the **Cu_2O_x** species (see above, Figure 2) did not exclude the possibility that a mono-μ oxo dicopper(II) species (**Cu_2O**) can be stabilized with the **BPMDP** system, we also tried to generate it with oxygen atom transfer (OAT) reagents. To this end, **2**-PF_6 was reacted with the OAT reagent iodosobenzene (PhIO) and nitrous oxide under exclusion of O_2 at 233 K, and the reaction was followed using UV/Vis spectroscopy and Cryo-UHR-ESI-MS. A temperature of 233 K was chosen because our previous study on the **bdpdz**/**bdptz** complexes showed that a **Cu_2O** species is stable at this temperature.

The reaction of an acetone solution of **2**-PF_6 with an excess of PhIO (10 eq.) at 233 K resulted in a color change from orange to dark green/brown. A UV/Vis spectrum with bands at 360 nm ($\varepsilon = 5200\ M^{-1}\ cm^{-1}$), a broad shoulder at 440 nm ($\varepsilon = 710\ M^{-1}\ cm^{-1}$) and a band at 615 nm ($\varepsilon = 140\ M^{-1}\ cm^{-1}$) was obtained (**Figure 8**, red). Similar results were obtained by reaction of **2**-PF_6 with N_2O at 233 K. When N_2O was introduced, the acetone solution of **2**-PF_6 changed its color from orange to green/brown within 30 min, and a UV/Vis spectrum with bands at 360 ($\varepsilon = 4000$), 440 ($\varepsilon = 650$) and 620 nm ($\varepsilon = 250\ M^{-1}\ cm^{-1}$) emerged (Figure 8, green). The obtained spectrum differs significantly from that of the **Cu_2O_2** complex **3**.

The observed bands at 360, 440, and 620 nm are in similar positions as in the **Cu_2O** complex of the **bdpdz**/**bdptz** system (370, 420, and 630 nm).[15] However, the extinction coefficients observed here are much smaller. Furthermore, the solution appears brownish; that is, the characteristic green color as described in the literature for **Cu_2O** species is not observed,[15,42–47] suggesting that this species might not have formed or is not stabilized as well as in the **bdpdz**/**bdptz** system. A further decrease of the intensity of the band at 615 nm is

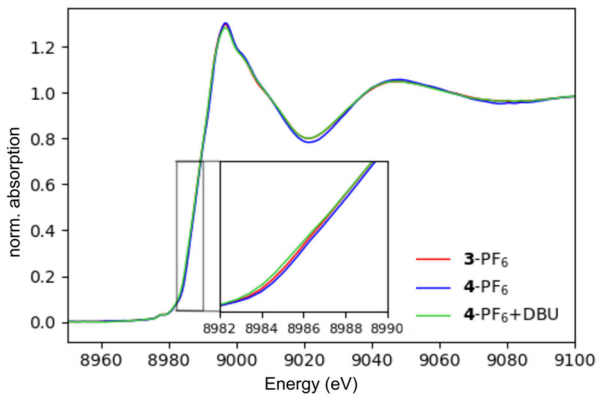

Figure 7. Cu K-edge XANES spectra of the initially measured μ-1,2 **Cu_2O_2** complex **3**-PF_6 (red) **2**-PF_6, of the **Cu_2OOH** complex **4**-PF_6 (blue) and after subsequent deprotonation of **4**-PF_6 with DBU (green).

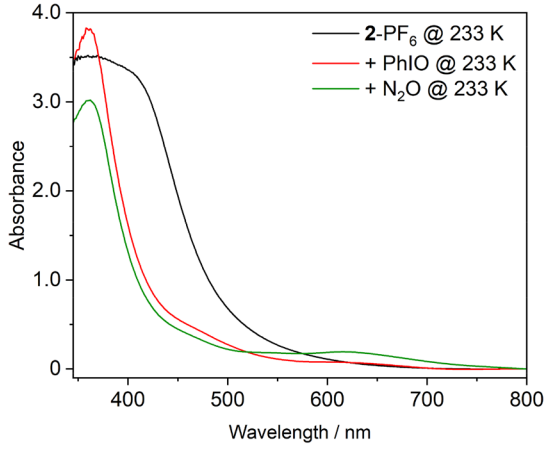

Figure 8. UV/Vis spectrum of an acetone solution of **2**-PF_6 (black), after reaction with PhIO at 233 K (red) or after reaction with N_2O at 233 K (green).

Research Article
doi.org/10.1002/ejic.202500286

observed upon warming of solution to room temperature (Figure S19 and S20, Supporting Information).

In order to obtain complementary information on that issue, Cryo-UHR-ESI-MS was employed. Upon reaction of **2**-PF_6 with PhIO at 233 K the [**Cu_2(BPMPD)O**]$^{2+}$ dication is found as the main species in the mass spectrum (*calc. m/z* 322.0562, *obs. m/z* 322.0570). The cutout of the cryo-ESI mass spectrum showing this species is reproduced in **Figure 9**. In addition, a [**Cu_2(BPMPD)OH**]$^{3+}$ complex (*calc. m/z* 215.0399, *obs. m/z* 215.0393) is visible, as well as the Cu(I) complex [**Cu_2(BPMPD)**]$^{2+}$ (*calc. m/z* 314.0587, *obs. m/z* 314.0580) (Section S7.3). Reaction of **2**-PF_6 with N_2O at 233 K led to comparable results (Section S7.4).

The fact that the **Cu_2O** complex is observed in the mass spectrum as the main species, however, does not constitute evidence that this intermediate is present in solution. Notably, for the **Cu_2OH** complex of our previously studied **MO8** system a **Cu_2O** species was observed in the mass spectrum as well, along with the Cu(I) and the μ-hydroxo complex.[16] Therefore, it is possible that addition of OAT reagents to the Cu(I) complex of the **BPMPD** system generates a hydroxo complex in a homogeneous solution that gets deprotonated in the gas phase Alternatively, a dicopper μ-hydroxo/hydroxo intermediate is formed in solution that is dehydrated in the gas phase, also leading to a **Cu_2O** species.[16] Both of these scenarios have been observed in the **MO8** system[16] and would in principle be compatible with the observed UV/Vis spectrum. (Figure 8). However, the UV/Vis spectrum obtained here differs from that of the μ-hydroxo complex **5** (Figure S21, Supporting Information).

We also made an attempt to generate a **Cu_2O** species by deprotonation of the **Cu_2OH** complex **5**-ClO_4 with 1.2 eq. DBU and investigated the reaction by means of UV/Vis spectroscopy. After addition of DBU and warming to rt, the **Cu_2OH** bands decreased and the solution changed its color from green to orange. The UV/Vis spectrum obtained looks very similar to that of the Cu(I)-complex **2**-PF_6 (Figure S23, Supporting Information). The previously investigated **MO8** system shows the same behavior toward DBU. In the case of **MO8** the formation of Cu(I) was confirmed by XAS.[16] We therefore assume that Cu(I) was also formed in the case of **BPMPD**.

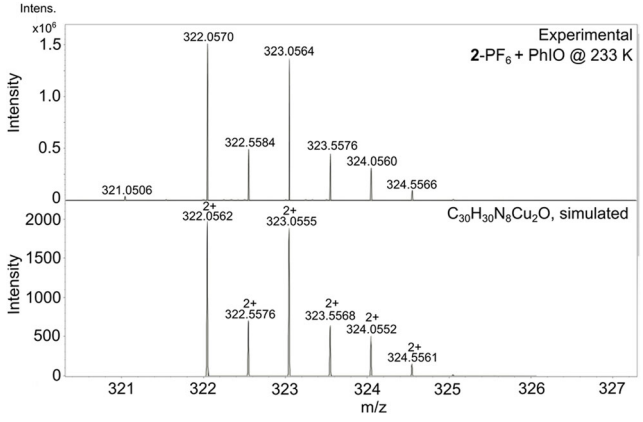

Figure 9. Cutout of the cryo-ESI mass spectrum obtained after reaction of **2**–PF_6 with PhIO at 233 K (top) and simulated spectrum of the **Cu_2O** complex (bottom).

3. Conclusion

In this work we have investigated the dinuclear Cu(I) system based on the ligand **BPMPD** with regard to its reactivity toward oxygen at low temperatures. The original, literature-known synthesis route of **BPMPD** was simplified, allowing easier access to this ligand. Reaction of **BPMDP** with the copper(I) precursors $[Cu(CH_3CN)_4]X$ (with $X = PF_{6-}$ or OTf^-) resulted in the new Cu(I) complexes [Cu_2(**BPMPD**)$(CH_3CN)_2$]$(X)_2$. Theoretical considerations, as well as the known crystal structure of the **Cu_2OH** complex of this system, indicated that a **Cu_2O_x** species in which Cu is pentacoordinated (i.e., **Cu_2O**, **Cu_2OOH** or μ-1,2 **Cu_2O_2**) is more likely than a hexacoordinate structure (i.e., side-on peroxo **Cu_2O_2**, bis-μ oxo **Cu_2O_2** or bis-μ hydroxo).

When O_2 is introduced into a solution of [Cu_2(**BPMPD**)$(CH_3CN)_2$]$(PF_6)_2$ at 203 K, a color change from orange to dark blue/purple is visible. UV/Vis, Cryo-UHR-ESI-MS, rRaman and XAS data indicate the formation of a μ-1,2 **Cu_2O_2** species. The **Cu_2O_2** species was examined with regard to its ability to oxygen transfer to dihydroanthracene (DHA) and a conversion of 14% (TON = 0.35) was observed.

Furthermore, it was investigated whether the μ-1,2 **Cu_2O_2** species **3**-PF_6 can be reversibly protonated. The reaction of **3**-PF_6 with [Lut-H][OTf] led to a green solution, and the UV/Vis and XAS data indicated the formation of a **Cu_2OOH** species **4**-PF_6. The addition of DBU to this solution resulted in the recovery of the original dark blue/purple color, as well as the original UV/Vis and XAS spectra, demonstrating that the **Cu_2O_2** species of the **BPMDP** system can be reversibly protonated. The **Cu_2OOH** species **4** can also be obtained by reaction of the **Cu_2OH** complex **5** with H_2O_2 at low temperatures.

Since the theoretical consideration of the system did not exclude the possibility of the formation of a **Cu_2O** species, we attempted to generate this species with the oxygen-atom transfer reagents PhIO and N_2O. The UV/Vis and Cryo-UHR ESI-MS data obtained suggest that such a species could possibly be present, but the UV/Vis spectrum indicates an incomplete reaction or instability of this species in the **BPMPD** system and is also compatible with a hydroxo complex as observed for the **MO8** system.[16] An attempt to deprotonate the **Cu_2OH** complex **5** to obtain a **Cu_2O** species resulted in the formation of a Cu(I)-complex, as observed before for the **MO8** system.[16]

In summary, we could show that variation of the chain length and type of *N*-donors in the side arms entails significant changes in reactivity toward oxygen compared to our previously investigated pyridazine-bridged dicopper complexes (**bdpdz**/**bdptz** and **MO8**). In particular, modifying the ligand design of these systems leads to different **Cu_2O_x** intermediates upon oxygenation; that is, **bdpdz**/**bdptz** → **Cu_2O**, **MO8** → **Cu_2OOH** and **BPMPD** → **Cu_2O_2**, the latter intermediate allowing reversible conversion to **Cu_2OOH**. Regarding the stability and formation of these species and the monooxygenation activities of the corresponding dicopper complexes, the present series of pyridazine-bridged systems thus provides another compelling example of structure-function correlation emerging from rational and systematic variation of the supporting ligand.

Acknowledgements

The authors thank CAU Kiel for the support of this research. The authors acknowledge DESY (Hamburg, Germany), a member of the Helmholtz Association HGF, for the provision of experimental facilities. Parts of this research were carried out at P65 beamline of Petra III and the authors would like to thank Gurman Singh, Edmund Welter and Sergiu Levcenco for their assistance. The authors are grateful to Yannik Appiarius for the GC-MS measurements. The authors would like to thank Tobias Engesser, Jan Krahmer and Kai Uwe Clausen for spectroscopic measurements and Melissa Teubner for her help on the resonance Raman spectroscopy. B.G.-L. gratefully acknowledges the Bundesministerium für Bildung und Forschung (BMBF) project 05K19GU5 for funding. S.B. gratefully acknowledges the Deutsche Forschungsgemeinschaft (DFG) for financial support under project RU 773/8–1.

Open Access funding enabled and organized by Projekt DEAL.

Conflict of Interest

The authors declare no conflict of interest.

Author Contributions

Alexander Stüber: formal analysis (lead); investigation (lead); writing—original draft (lead). **Ramona Jurgeleit**: investigation (equal); writing—original draft (equal). **Kira Berger**: formal analysis (equal); investigation (equal). **Benjamin Grimm-Lebsanft**: investigation (equal). **Sören Buchenau**: investigation (supporting). **Laura Senft**: investigation (supporting). **Christian Näther**: investigation (supporting). **Ivana Ivanović-Burmazović**: conceptualization (supporting); validation (supporting); writing—review and editing (supporting). **Michael Rübhausen**: conceptualization (supporting); investigation (supporting); methodology (supporting). **Maria A. Naumova**: investigation (equal); methodology (supporting); writing—original draft (supporting); writing—review and editing (supporting). **Felix Tuczek**: conceptualization (lead).

Data Availability Statement

The data that support the findings of this study are available in the supplementary material of this article.

Keywords: copper · extended X-ray absorption fine structure spectroscopy · metalloenzymes · oxygenation · Raman spectroscopy

[1] E. I. Solomon, D. E. Heppner, E. M. Johnston, J. W. Ginsbach, J. Cirera, M. Qayyum, M. T. Kieber-Emmons, C. H. Kjaergaard, R. G. Hadt, L. Tian, *Chem. Rev.* **2014**, *114*, 3659.
[2] L. M. Mirica, X. Ottenwaelder, T. D. P. Stack, *Chem. Rev.* **2004**, *104*, 1013.
[3] W. Kaim, J. Rall, *Angew. Chem. Int. Ed. Engl.* **1996**, *35*, 43.
[4] M. Rolff, J. Schottenheim, H. Decker, F. Tuczek, *Chem. Soc. Rev.* **2011**, *40*, 4077.
[5] B. E. R. Snyder, M. L. Bols, R. A. Schoonheydt, B. F. Sels, E. I. Solomon, *Chem. Rev.* **2018**, *118*, 2718.
[6] J. S. Woertink, P. J. Smeets, M. H. Groothaert, M. A. Vance, B. F. Sels, R. A. Schoonheydt, E. I. Solomon, *Proc. Natl. Acad. Sci.* **2009**, *106*, 18908.
[7] A. Rajeev, T. P. Mohammed, A. George, M. Sankaralingam, *Chem. Rec.* **2025**, *25*, e202400186.
[8] C. Noß, R. Göttlich, S. Schindler, *Chem. Eur. J.* **2023**, *29*, e202301142.
[9] L. Marais, J. Burés, J. H. L. Jordaan, S. Mapolie, A. J. Swarts, *Org. Biomol. Chem.* **2017**, *15*, 6926.
[10] A. Koch, T. A. Engesser, F. Tuczek, *Organometallics* **2023**, *42*, 1774.
[11] M. L. Perrone, E. Lo Presti, S. Dell'Acqua, E. Monzani, L. Santagostini, L. Casella, *Eur. J. Inorg. Chem.* **2015**, *2015*, 3493.
[12] L. Marais, H. C. Vosloo, A. J. Swarts, *Coord. Chem. Rev.* **2021**, *440*, 213958.
[13] J. Manzur, A. M. García, R. Letelier, E. Spodine, O. Peña, D. Grandjean, M. M. Olmstead, B. C. Noll, *J. Chem. Soc., Dalton Trans.* **1993**, 905.
[14] A. M. Barrios, S. J. Lippard, *J. Am. Chem. Soc.* **1999**, *121*, 11751.
[15] R. Jurgeleit, B. Grimm-Lebsanft, B. M. Flöser, M. Teubner, S. Buchenau, L. Senft, J. Hoffmann, M. Naumova, C. Näther, I. Ivanović-Burmazović, M. Naumova, M. Rübhausen, F. Tuczek, *Angew. Chem. Int. Ed.* **2021**, *60*, 14154.
[16] A. Stüber, R. Jurgeleit, B. Grimm-Lebsanft, S. Buchenau, I. Kellner, Y. Appiarius, C. Näther, J. Krahmer, I. Ivanović-Burmazović, M. Rübhausen, M. A. Naumova, F. Tuczek, *Chem. Eur. J.* **2025**, *0*, e202501659.
[17] H.-G. Korth, P. Mulder, *J. Org. Chem.* **2020**, *85*, 2560.
[18] Q.-F. Chen, K.-L. Xian, H.-T. Zhang, X.-J. Su, R.-Z. Liao, M.-T. Zhang, *Angew. Chem. Int. Ed.* **2024**, *63*, e202317514.
[19] R. Jurgeleit, *Ph.D. thesis*, **2021**, Christian-Albrechts-Univerität Kiel.
[20] K. Berger, *Master thesis*, **2022**, Christian-Albrechts-Univerität zu Kiel.
[21] J. C. Deàk, L. K. Iwaki, D. D. Dlott, *J. Phys. Chem. A* **1998**, *102*, 8193.
[22] C. E. Elwell, N. L. Gagnon, B. D. Neisen, D. Dhar, A. D. Spaeth, G. M. Yee, W. B. Tolman, *Chem. Rev.* **2017**, *117*, 2059.
[23] N. Kindermann, E. Bill, S. Dechert, S. Demeshko, E. J. Reijerse, F. Meyer, *Angew. Chem. Int. Ed.* **2015**, *54*, 1738.
[24] P. Vanelderen, R. G. Hadt, P. J. Smeets, E. I. Solomon, R. A. Schoonheydt, B. F. Sels, *J. Catal.* **2011**, *284*, 157.
[25] K. E. Dalle, T. Gruene, S. Dechert, S. Demeshko, F. Meyer, *J. Am. Chem. Soc.* **2014**, *136*, 7428.
[26] N. Kindermann, S. Dechert, S. Demeshko, F. Meyer, *J. Am. Chem. Soc.* **2015**, *137*, 8002.
[27] C.-J. Spyra, D. Hiller, K. A. Eisenlohr, S. Dechert, S. Demeshko, D. Bhattacharya, J. Lücken, M. C. Holthausen, F. Meyer, *Angew. Chem. Int. Ed.* **2025**, *64*, e202416022.
[28] H. Börzel, P. Comba, K. S. Hagen, M. Kerscher, H. Pritzkow, M. Schatz, S. Schindler, O. Walter, *Inorg. Chem.* **2002**, *41*, 5440.
[29] P. K. Hota, A. Jose, S. Panda, E. M. Dunietz, A. E. Herzog, L. Wojcik, N. Le Poul, C. Belle, E. I. Solomon, K. D. Karlin, *J. Am. Chem. Soc.* **2024**, *146*, 13066.
[30] N. Kindermann, C.-J. Günes, S. Dechert, F. Meyer, *J. Am. Chem. Soc.* **2017**, *139*, 9831.
[31] D. A. Quist, M. A. Ehudin, A. W. Schaefer, G. L. Schneider, E. I. Solomon, K. D. Karlin, *J. Am. Chem. Soc.* **2019**, *141*, 12682.
[32] A. Brinkmeier, R. A. Schulz, M. Buchhorn, C.-J. Spyra, S. Dechert, S. Demeshko, V. Krewald, F. Meyer, *J. Am. Chem. Soc.* **2021**, *143*, 10361.
[33] M. Mahroof-Tahir, K. D. Karlin, *J. Am. Chem. Soc.* **1992**, *114*, 7599.
[34] E. Borghi, L. Casella, *Phys. Chem. Chem. Phys.* **2010**, *12*, 1525.
[35] F. G. Bordwell, J. Cheng, G. Z. Ji, A. V. Satish, X. Zhang, *J. Am. Chem. Soc.* **1991**, *113*, 9790.
[36] K. D. Karlin, P. Ghosh, R. W. Cruse, A. Farooq, Y. Gultneh, R. R. Jacobson, N. J. Blackburn, R. W. Strange, J. Zubieta, *J. Am. Chem. Soc.* **1988**, *110*, 6769.
[37] N. N. Murthy, M. Mahroof-Tahir, K. D. Karlin, *Inorg. Chem.* **2001**, *40*, 628.
[38] K. Itoh, H. Hayashi, H. Furutachi, T. Matsumoto, S. Nagatomo, T. Tosha, S. Terada, S. Fujinami, M. Suzuki, T. Kitagawa, *J. Am. Chem. Soc.* **2005**, *127*, 5212.
[39] S. Teramae, T. Osako, S. Nagatomo, T. Kitagawa, S. Fukuzumi, S. Itoh, *J. Inorg. Biochem.* **2004**, *98*, 746.

[40] L. Li, A. A. Narducci Sarjeant, M. A. Vance, L. N. Zakharov, A. L. Rheingold, E. I. Solomon, K. D. Karlin, *J. Am. Chem. Soc.* **2005**, *127*, 15360.
[41] D. E. Root, M. Mahroof-Tahir, K. D. Karlin, E. I. Solomon, *Inorg. Chem.* **1998**, *37*, 4838.
[42] P. Haack, C. Limberg, *Angew. Chem. Int. Ed.* **2014**, *53*, 4282.
[43] K. D. Karlin, Y. Gultneh, J. C. Hayes, J. Zubieta, *Inorg. Chem.* **1984**, *23*, 519.
[44] P. Haack, A. Kärgel, C. Greco, J. Dokic, B. Braun, F. F. Pfaff, S. Mebs, K. Ray, C. Limberg, *J. Am. Chem. Soc.* **2013**, *135*, 16148.
[45] P. Haack, C. Limberg, K. Ray, B. Braun, U. Kuhlmann, P. Hildebrandt, C. Herwig, *Inorg. Chem.* **2011**, *50*, 2133.
[46] H. V. Obias, Y. Lin, N. N. Murthy, E. Pidcock, E. I. Solomon, M. Ralle, N. J. Blackburn, Y.-M. Neuhold, A. D. Zuberbühler, K. D. Karlin, *J. Am. Chem. Soc.* **1998**, *120*, 12960.
[47] N. Kitajima, T. Koda, Y. Moro-oka, *Chem. Lett.* **1988**, *17*, 347.

Manuscript received: June 9, 2025
Revised manuscript received: July 30, 2025
Version of record online: August 13, 2025